한국해양공학회지 제21권 제6호, pp 26-33, 2007년 12월 (ISSN 1225-0767)

Finite Element Simulation of Elastic Wave Propagation in a Concrete Plate - Modeling and Damage Detection

JINHO WOO*, WON-BAE NA*, JEONG-TAE KIM*, AND HYUN-MAN CHO*
*Department of Ocean Engineering, Pukyong National University, Busan, Korea

KEY WORDS: Finite element simulation, Elastic wave, Damage detection

ABSTRACT: *Finite element simulation of elastic wave propagation in a concrete plate was carried out to investigate its modeling and damage detection procedures. For the numerical stability three criteria were introduced and tested. With a proper element size and time increment, two different kinds of damage scenarios (crack and deterioration) were applied to verify the feasibility of the finite element simulation. It is shown that the severities of those damages are sensitive to the received displacement signals.*

1. Introduction

Nondestructive testing (NDT) techniques based on ultrasonic wave propagation are widely used for testing structures and mechanical components (Na and Kang, 2006). These experimental techniques are mainly used for the evaluation of mechanical properties and material deteriorations. Initially, steel was the main target material for the testing but nowadays concrete gets benefit from these testing techniques. In addition to the ultrasonic waves, elastic waves with less frequency have been also used for concrete testing. A representative testing technique is the impact echo method mainly developed by Sansalone and Carino (1987), Sansalone et al. (1987), Lin and Sansalone (1992), and Sansalone (1997). During the development of the impact echo method, finite element method (FEM) was used to simulate the impact echo response of structures. For example, starting from a simple wave propagation problem in a plate, Sansalone and Carino (1987) simulated planar defects in plates. They concluded that the results obtained from FE (finite element) solutions helped in developing a theoretical basis for utilizing the impact echo method for detecting defects or anomalies in heterogeneous solids such as concrete. Finally, Sansalone (1997) summarized the works carried out to successfully implement the impact echo method on reinforced concrete (RC) structures and pointed out the importance of using FE based computer models for simulating the impact echo response of structures. These FE models permitted them to study transient stress wave propagation in bounded solids with or without defects.

However, the finite element simulation of elastic wave propagation with a relatively high frequency such as ultrasonic wave is quite challenged. In the FE simulation, high frequency wave means that the element size should be small enough to represent the wavelength. In other words, the solution time becomes incredibly large. Thus, other numerical methods such as boundary element method (BEM), semi-analytical finite element method (SAFEM), elastodynamic finite integration technique (EFIT), and distributed point source method (DPSM) have been simultaneously developed (Hayashi et al., 2006; Schubert, 2004; Banerjee and Kundu, 2006). These methods have their own development stages for elastic wave simulation with weak and strong points. Thanks to modern development of computer hardware and software such as ABAQUS/Explicit, ANSYS LS-DYNA, FEMLAB, and MARC, large amount of numerical calculations become possible. Thus, many investigators continuously use FE simulation for elastic wave propagation over high frequency ranges (Nieuwenhuis et al., 2005; Butėnas and Kažys, 2006; Ichchou et al., 2007; Klenow et al., 2007; Abdullah et al., 2007).

This study is one of those investigations. This study concerns how the finite element model should be constructed and how the internal damages become detectable under a certain parameter. For the purpose, first, a concrete plate is modeled using 2-D plane element, a tone-burst Gaussian displacement loading is applied to axial direction, two nodal points are selected as numerical sensors, and two damage scenarios are applied to verify the feasibility of the finite

교신저자 나원배: 부산광역시 남구 대연3동 599-1번지
051-620-6225 wna@pknu.ac.kr

element simulation. Second, three criteria for numerical stability are introduced and tested. Finally, the sensitivity of element size, time increment, and the severity of damages on the received displacement signals are reported and discussed. For the finite element simulation, the general purpose finite element software, ANSYS LS-DYNA is used.

This study is the initial part of developing a reliable nondestructive testing technique for a large sized concrete harbor structures that suffered from deteriorations and challenged by the port remodeling project in Korea Republic. A series of advanced research results will follow as the subsequent materials in the near future.

2. Wave Propagation Analysis by FEM

For a structure modeled with finite elements, the solution of the governing dynamic equilibrium equations is usually handled by the mode-superposition and direct integration method. The solution procedure of the mode-superposition method takes advantages of the property matrices, and it is not applicable to nonlinear problems. In principle, the coupled equations of motion can be uncoupled using modal transformation. The individual modal responses of the uncoupled equations are solved for each mode of vibration and the total response is obtained upon superposition. This procedure is most useful when the response can be evaluated by considering the first few modes of vibration of the structure (Bathe, 1996).

In the direct integration method, the response history of the structure is obtained using a numerical step-by-step integration procedure. Unlike the mode-superposition method, the equations are not transformed into modal coordinates; hence, it can be also applied to systems with non-linearity. The utilization of the step-by-step numerical integration procedure is generally classified into two integration schemes: implicit and explicit.

In an implicit integration schemes such as Wilson-Θ or Newmark method, the displacement response is found from expressions that satisfy equilibrium at $'t+\Delta t'$. This results in an inversion requirement of an effective stiffness matrix which is not diagonal but symmetric (invertible) thus making the computation highly expensive, especially for large degree of freedom (DOF) systems. Since the equilibrium equation is always satisfied for the time step that the response is sought, this integration scheme is unconditionally stable.

However, in an explicit scheme such as the central difference method, dynamic equilibrium is considered at time $'t'$ to evaluate the response at time $'t+\Delta t'$. This leads to the inversion of an effective mass matrix, which is symmetric and diagonal, if the lumped mass matrix formulation is utilized, thus making the inversion process much easier. This fact of explicit integration makes it more attractive to use in the large DOF systems. However, the drawback of explicit integration schemes is the conditional stability of the solution. Therefore, there is a maximum integration time step limitation on the explicit integration schemes. In addition, the displacement response will be exact for constant accelerations. Therefore, to obtain accurate dynamic response, a small time increment has to be selected so that accelerations will be small within the time step. Because of its requirement of smaller time increments than implicit integration schemes, more increments are needed for a specific problem. However, since there is no matrix inversion process involving during each increment, the total cost of analysis is usually much cheaper, especially for a large DOF system.

An important consideration in the explicit integration scheme is the selection of the time step. If the time increment (step) is greater than a critical value, Δt_c, there is a possibility that the numerical integration will become unstable. Therefore, explicit integration schemes are said to be "conditionally stable." This limiting time step is called the stability limit. The limit is defined in terms of the highest frequency of the FE system and written as:

$$\Delta t_c = \frac{2}{\omega_{\max}} = \frac{T_{\min}}{\pi} \tag{1}$$

where $\omega_{\max}$ is the highest frequency and $T_{\min}$ is the corresponding minimum period of the FE system. However, computing the exact value of $\omega_{\max}$ or $T_{\min}$ may not be computationally feasible. Instead, the use of the highest frequency of each element ($\omega^e_{\max}$) in the model can be an efficient, conservative approximation (Bathe, 1996). Thus, the estimate of the stability limit can be defined using the critical element length (l_c) and the longitudinal wave speed (C_l) of the material as follows:

$$\Delta t_c = \frac{l_c}{C_l} \tag{2}$$

This stability limit enables one to select an appropriate time step to get an accurate response calculation. If a time step larger than Δt_c is used, the integration may become unstable in a divergent solution.

Alternative empiric formula for the stability check is used by Hora and Michalek (2000) as below:

$$l_c = \frac{\lambda_{\min}}{20} \tag{3}$$

where, $\lambda_{\min}$ is the smallest wavelength. Eq. 2 and Eq. 3 can be rewritten as follows:

$$\Delta x \leq l_c = \frac{\lambda_{\min}}{20} \tag{4}$$

$$\Delta t \leq \Delta t_c = \frac{l_c}{C_l} \tag{5}$$

where, Δx is the element size and Δt is the time increment for wave propagation simulation. These two equations can be combined into one equation using the term Courant number as below:

$$cr = \frac{C_l(\Delta t)}{(\Delta x)} < 1 \tag{6}$$

In explicit integration schemes, another way of checking the numerical stability is to monitor the energy balance of the finite element model. Total energy balance and the gradient of the internal energy are significant parameters to monitor the stability. A divergence solution usually result in an unrealistic energy shift in the system, which will denote the selection of an incorrect time increment (Yaman et al., 2006).

3. Finite Element Models

The typical ultrasonic testing unit for the pitch and catch mode is shown in Fig. 1. Figure 1(a) shows the unit having one transmitter and one receiver, and Fig. 1(b) shows the unit having one transmitter and two receivers. Based on the pitch and catch mode shown in Fig. 1(b), the finite element models and simulation were designed in the study.

The target structure is a thick plate as shown in Fig. 2(a). The length is 400 mm and the height is 40 mm. Four nodes-plane strain element is used for ANSYS LS-DYNA, a finite element program. For a proper element size and time increment, four different selections are made as shown in Table 1. First two selections only satisfy the criterion shown in Eq. (6). The third selection satisfies the criteria shown in Eqs. (5) and (6), and the last selection satisfies all the criteria shown in Eqs. (4), (5), and (6). Those selections are intentionally made to investigate how the element size and time increment affect the finite element simulation. In other words, they are made to investigate how the violations of those three criteria affect the finite element simulations.

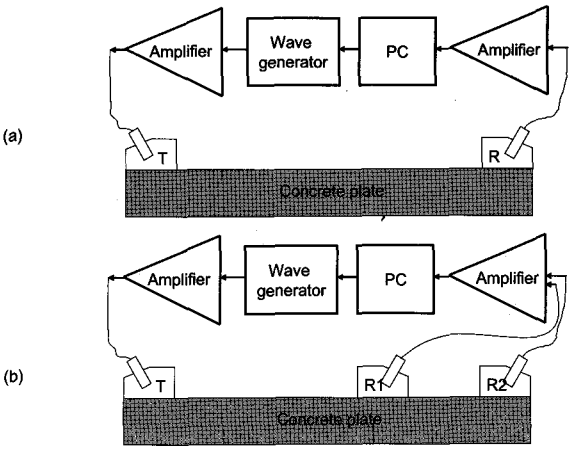

Fig. 1 Typical ultrasonic testing units for the pitch and catch mode: (a) one transmitter and one receiver, (b) one transmitter and two receivers

For the model, boundary conditions are made to minimize the boundary effects; hence, only two nodal points in the middle edges are constrained as shown in Fig. 2(a). Loading is a tone-burst Gaussian signal with six cycles over its duration as shown in Fig 3. The shape of the wave packet window is selected as Gaussian because the Gaussian function is an ideal window for a narrow band signal, having the same shape, without slope lobes, in the frequency domain. Total duration time is 0.15 msec and the frequency of the carrier wave is fixed to 50 kHz, which is a proper ultrasonic pulse frequency for the concrete inspection. The pulse is given as displacement loading conditions and the amplitude of the pulse is selected as 1 mm. The actual displacement of the displacement field that occurs during an ultrasonic testing is known to be very small, but actual displacement amplitudes are not defined here. The loading is excited on the excitation point in the x direction, as shown in Fig. 2 and other two points denoted by sensor 1 and sensor 2 are the points at which data are collected, as described in Table 3. The material properties and their corresponding acoustic properties are shown in Table 4. Linear elastic isotopic material is assumed for the modeling.

Two different kinds of damage scenarios are made as shown in Fig. 2(b), Fig. 2(c), and Table 5. Damage 1 (crack) is simulated by applying geometric constraints in corresponding nodal points. The depth of crack (a) varies from 2 to 8 mm with 2 mm intervals; hence, total four crack depths are considered. The crack is located from 4 mm below the top surface of the plate. Damage 2 is (deterioration) is simulated by reducing the half of Young's modulus on targeted elements. The width of deteriorated zone is fixed to 8mm and

the depth (b) is varied from 2 to 8 mm with 2 mm intervals as damage 1. The zone is also located from 4 mm below the top surface. The severities of the crack depth and the deteriorated regions are defined in Table 6.

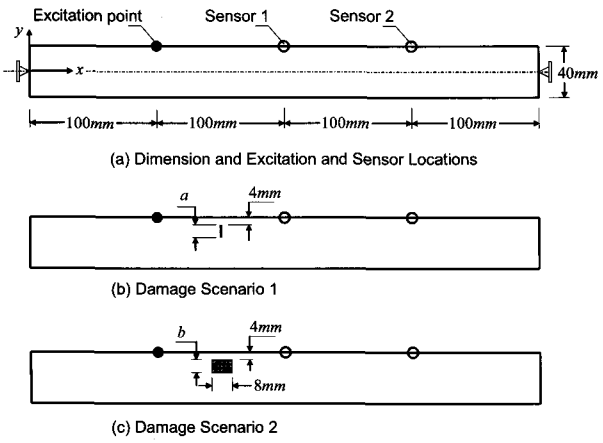

Fig. 2 Structure dimension and locations of excitation and sensors (a), damage scenario 1 (b), and damage scenario 2 (c)

Table 1 Selection of element size and time increment

Calculated critical values			Selected element size and time increment				Courant number	
$\lambda_{\min}$ (mm)	l_c (mm)	Δt_c (sec)	Δx (mm)	Check	Δt (mm)	Check	cr	Check
67	3.35	1E-6	20	NG	4.76E-6	NG	0.7973	OK
			10	NG	2.35E-6	NG	0.7872	OK
			4	NG	9.46E-7	OK	0.7923	OK
			2	OK	4.68E-7	OK	0.7839	OK

Table 2 FE model for element size and time increment

Element size (mm)	No of elements	No of time increment	Time increment (sec)
20	40	210	4.76E-6
10	160	425	2.35E-6
4	1000	1057	9.46E-7
2	4000	2139	4.68E-7

Table 3 Nodal points for wave excitation and receptions

Element size (mm)	No of elements	Nodal points		
		Excitation	Receiver 1	Receiver 2
20	40	39	34	29
10	160	76	66	56
4	1000	187	162	137
2	4000	372	322	272

4. Effect of Element Size and Time Increment

The four different element sizes and time increments as explained in Table 2 were used for finite element simulation. From the explicit finite element analysis, displacement (UX) and Stress (SX) in the direction of x axis were obtained as time signals. As explained earlier, those signals were captured at the two receiving points (sensor 1 and sensor 2). Figure 4 shows UX at sensor 1 and Fig. 5 shows UX at sensor 2. Over whole time period (1 msec) only initial parts are shown here. Other later captured signals are quite complex because of

Table 4 Material properties of target concrete plate

Young's modulus	28.028E6 kg/sec^{2}mm
Poisson's ratio	0.2
Density	2.5E-6 kg/mm^3
P wave velocity	3.35E3 m/sec
S wave velocity	2.16E3 m/sec

Table 5 Damage scenarios

Damage Scenario	Description	Damage depth
1	Crack	a = 2, 4, 6, 8 mm, respectively
2	Deterioration	b = 2, 4, 6, 8 mm, respectively

Table 6 Severity of the crack depth and the deteriorated regions

Damage scenario 1 (beam depth = 40 mm)		Damage scenario 2 (total beam area = 16000 mm^2)		
Depth (a)	Severity	Depth (b)	Area	Severity
2 mm	5%	2 mm	16 mm^2	0.1 %
4 mm	10%	4 mm	32 mm^2	0.2 %
6 mm	15%	6 mm	48 mm^2	0.3 %
8 mm	20%	8 mm	64 mm^2	0.4 %

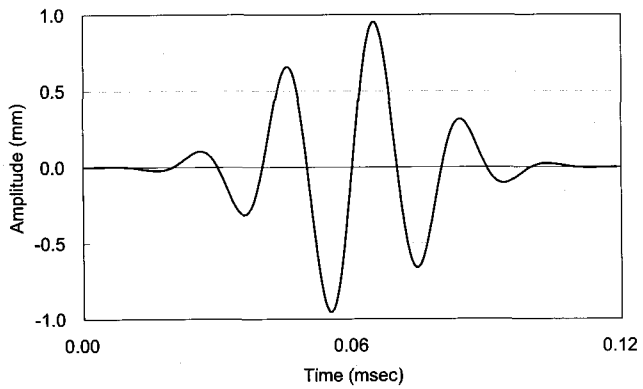

Fig. 3 Excitation signal

reflection and refraction of elastic waves on the boundary conditions. It is shown in Figs. 4 and 5 that the arrived signals at sensor 1 has less dispersive than those at sensor 2 because the excitation point is closer to sensor 1. Similar observation is made for SX signals as shown in Figs. 6 and 7. Besides, it is shown in all the four figures that the element size is critical to simulate the elastic wave propagation. Large element sizes (10x10 and 20x20) cannot simulate the correct wave pattern. The total energy balance is another parameter to monitor the numerical stability. It is shown in Fig. 8 that 2 mm and 4 mm sized elements have more numerical stability. Between 2 mm and 4 mm sized elements, the first one gives closer representation of the excitation signal as shown in Fig. 4. In addition, in practice, the actual stable time increment is recommended by dividing the critical element size (l_c) by $\sqrt{3}$, which means 1.93 mm in our case (Butėnas, and Kažys, 2006). Thus, the element size of 2 mm and the time increment of 4.68E-7 sec are selected for the remained finite element simulation. As checked in Table 1, those size and increment satisfy the three criteria. Figures. 9 and 10 show the time signals of UX and SX over the whole duration.

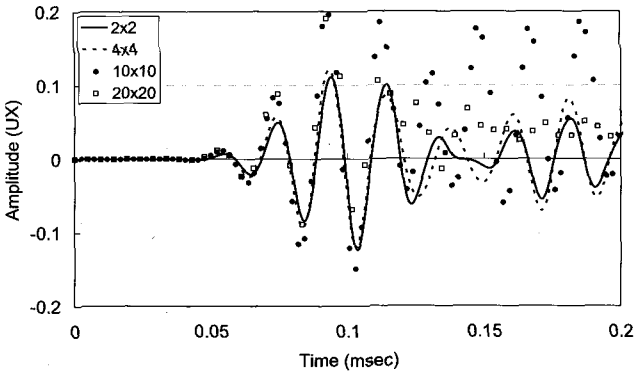

Fig. 4 Displacement (UX) signals (initial parts) from sensor 1

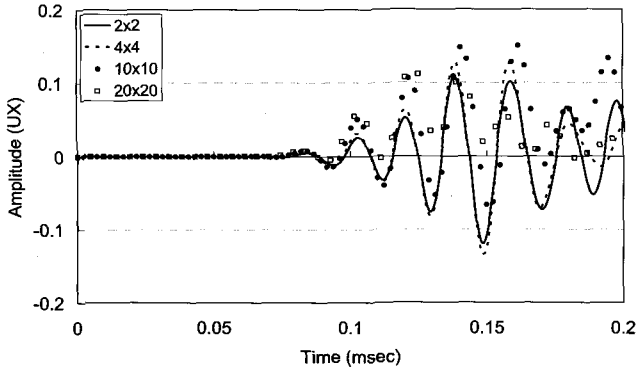

Fig. 5 Displacement (UX) signals (initial parts) from sensor 2

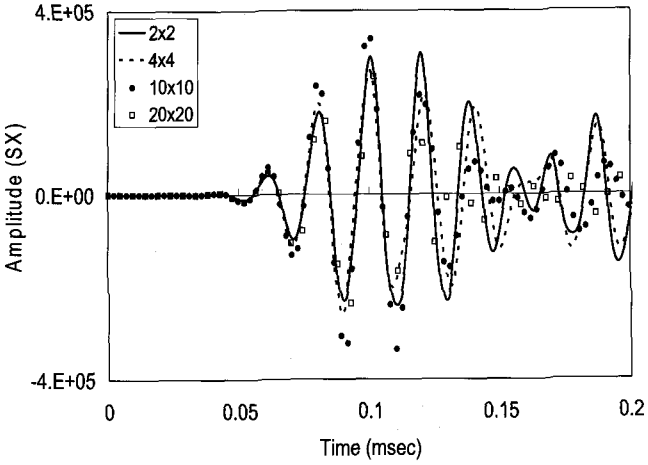

Fig. 6 Stress (SX) signals (initial parts) from sensor 1

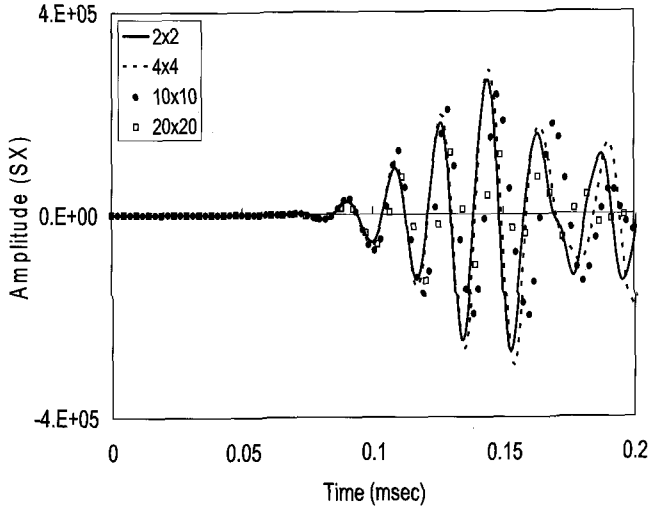

Fig. 7 Stress (SX) signals (initial parts) from sensor 2

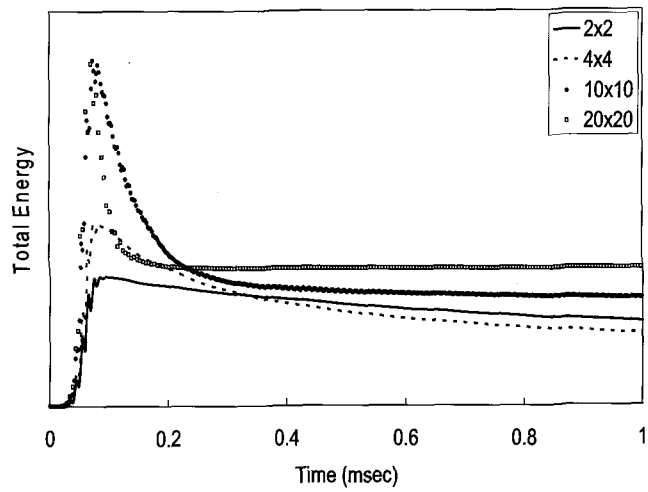

Fig. 8 Total energy of each model

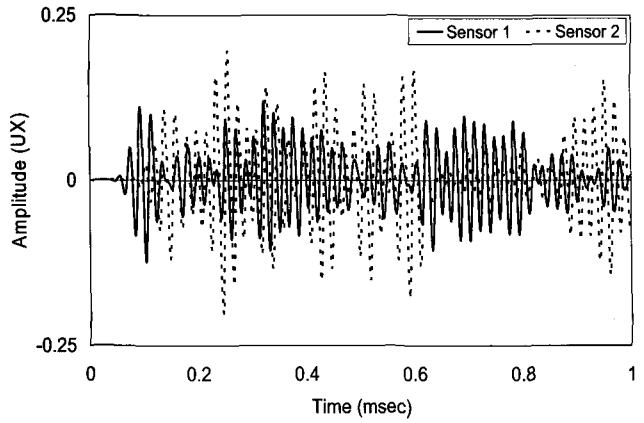

Fig. 9 Displacement signals (UX) from sensor 1 and sensor 2

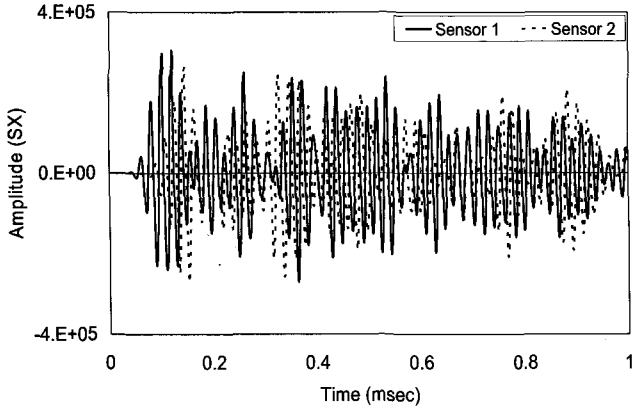

Fig. 10 Stress signals (SX) from sensor 1 and sensor 2

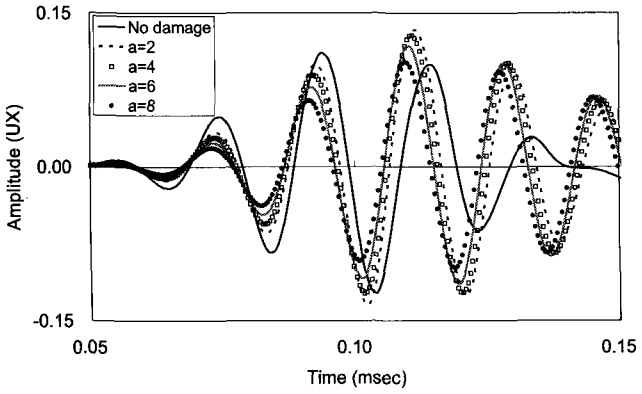

Fig. 11 Displacement signals (initial parts) from sensor 1, for each damage case of damage scenario 1

5. Damage Detection

To see how the received signals detect the damages, Figs. 11 to 15 are obtained. Figure 11 shows the displacement signals captured at sensor 1. As shown, the severity of damage 1 (crack) is well quantified in terms of frequency shift and amplitude change. The signals received from sensor 2 also show the severity of damage 1 as shown in Fig. 12. In the case of the damage 2 (deterioration), it is shown in Fig. 13 that sensor 1 catches the signal changes (amplitude changes)

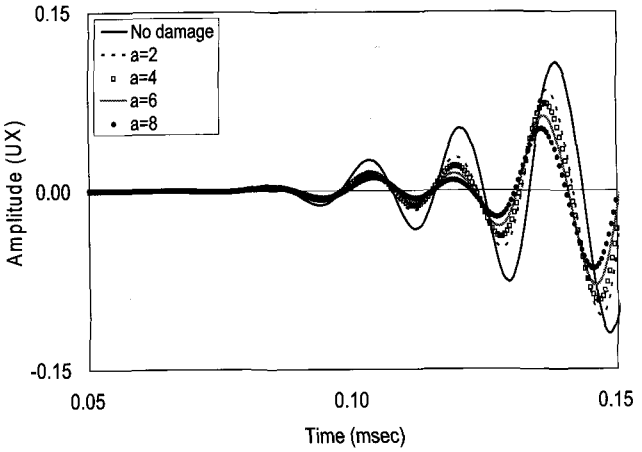

Fig. 12 Displacement signals (initial parts) from sensor 2, for each damage case of damage scenario 1

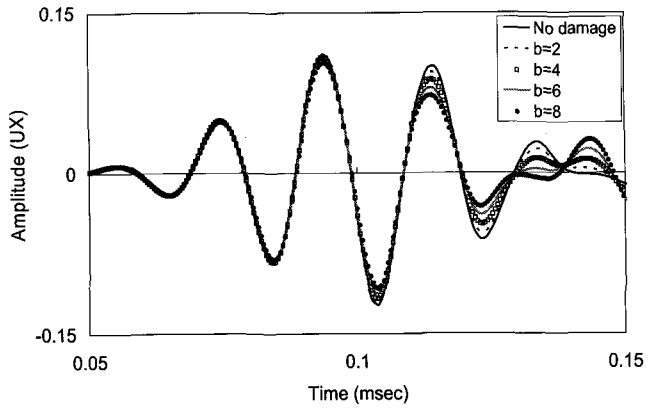

Fig. 13 Displacement signals (initial parts) from sensor 1, for each damage case of damage scenario 2

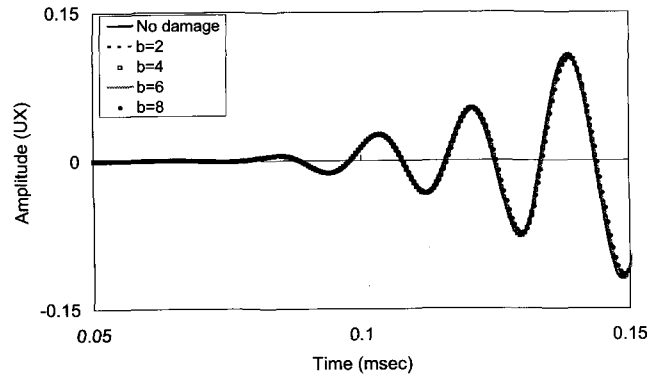

Fig. 14 Displacement signals (initial parts) from sensor 2, for each damage case of damage scenario 2

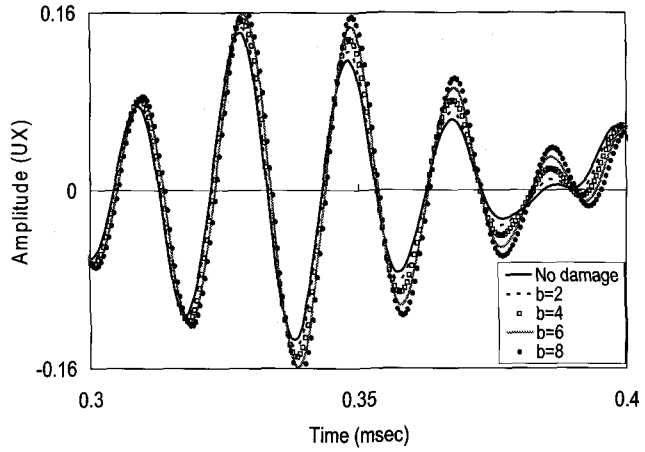

Fig. 15 Displacement signals (intermediate parts) from sensor 2, for each damage case of damage scenario 2

due to the damage. However, the signals received from sensor 2 does not show an evident clue for signal changes, as shown in Fig. 14. It is noted that those investigated signals are all the initial parts of the signals since those signals have less dispersive patterns. For a whole signals, the damage 2 is detectable over intermediate time domain from sensor 2, as shown in Fig. 15.

The previous detection is mainly based on the baseline signals that come from the damage free case. Based on the signals, the damage detections can be operated. Signal processing such as FFT (Fast Fourier Transform) and Wavelet transform can be used for the further analysis (Na et al., 2006). However, in the study, those analyses are not included.

6. Conclusion

A concrete plate was modeled by finite element simulation. For the simulation, a tone burst Gaussian displacement loading condition was applied to the top surface of the plate and two sensor locations were made to capture the elastic waves. For a proper simulation, four element sizes and time increments were considered, and tested. Among them, the element size of 2 mm was selected for the damage detection simulations since it satisfies three numerical stability criteria. Two damage scenarios (crack and deterioration) were made and the distinct damage severities were considered for each scenario. From the received signals from sensor 1 and sensor 2, the severities of each damage scenario were successfully distinguished. This study shows the sensitivity of element size and time increment on wave propagation, and the severities of damages on received signals. It is shown that the elastic wave propagation with a relatively high frequency can be simulated and the severities of damages are detectable.

Acknowledgement

This work was financially supported by Port Remodeling Project under Ministry of Maritime Affairs and Fisheries in 2007.

References

Abdullah, E., Ferrero, J.F., Barrau, J.J. and Mouillet, J.B. (2007). "Development of A New Finite Element for Composite Delamination Analysis", Composites Science and Technology, Vol 67, pp 2208-2218.

Banerjee, S. and Kundu, T. (2006). "Elastic Wave Propgationin Sinusoidally Corrugated Waveguides", Journal of the Acoustical Society of America, Vol 119, pp 2006-2017.

Bathe, K.J. (1996). Finite Element Procedure, Prentice Hall, New Jersey.

Butėnas, G. and Kažys, R. (2006). "Investigation of Time-Reversal Approach for Detection and Characterization of Ultrasonic Defects in Dispersive Plates", Ultragarsas, Vol 4, pp 34-39.

Hayashi, T., Tamayama, C. and Murase, M. (2006). "Wave Structure Analysis of Guided Waves in a Bar with an Arbitrary Cross-Section", Ultrasonics, Vol 44, pp 17-24.

Hora, P. and Michalek, J. (2000). "Numerical Modeling of Dispersion Phenomena in Thick Plate", Experimental Stress Analysis, the 38th International Conference, Brno, Brno University of Technology, 95-102.

Ichchou, M.N., Akrout, S. and Mencik, J.M. (2007). "Guided Waves Group and Energy Velocities Via Finite Elements", Journal of Sound and Vibration, Vol 305, pp 931-944.

Klenow, B., Niseworger, A., Batra, R.C. and Brown, A. (2007). "Reflection and Transmission of Plane Waves at an Interface Between Two Fluids", Computers and Fluids, Vol 36, pp 1298-1306.

Lin, Y. and Sansalone, M. (1992). "Transient Respone of Thick Circular and Square Bars Subjected to Transverse Elastic Impact", Journal of the Acoustical Society of America, Vol 92, pp 885-892.

Na, W.B. and Kang, D.B. (2006). "Effect of Surface Condition and Corrosion-Induced Defect on Guided Wave Propagation in Reinforced Concrete", Journal of Ocean Engineering and Technology, Vol 20, pp 1-6.

Na, W.B., Kim, J.T. and Ryu, Y.S. (2006). "Guided-Waves-Based Mortar-Filled Steel Pipe Inspection Using EMAT and Wavelet Transform", Journal of Ocean Engineering and Technology, Vol 20, pp 8-15.

Nieuwenhuis, J.H., Neumann, J.J., Greve, D.W. and Oppenheim, I.J. (2005). "Generation and Detection of

Guided Waves Using PZT Wafer Transducers", IEEE Transactions of Ultrasonics, Ferroelectrics, and Frequency Control, Vol 52, pp 2103-2111.

Sanalone, M. (1997). "Impact-Echo: The Complete Story", ACI Structural Journals, Vol 94, pp 777-786.

Sanalone, M. and Carino, N.J. (1987). "Transient Impact Response of Plates Containing Flaws", Journal of the National Bureau of Standards, Vol 92, pp 369-381.

Sansalone, M., Carino, N.J. and Hsu, N.N. (1987). "A Finite Element Study of Transient Wave Propagation in Plates", Journal of National Bureau of Standards, Vol 92, pp 267-278.

Schubert, F. (2004). "Numerical Time-Domain of Linear and Nonlinear Ultrasonic Wave Propagation using Finite Integration Techniques-Theory and Applications", Ultrasnics, Vol 42, pp 221-229.

Yaman, I.O., Akbay, Z. and Aktan, H. (2006). "Numerical Modelling and Finite Element Analysis of Wave Propagation for Ultrasonic Pulse Velocity Testing of Concrete", Computers and Concrete, Vol 3, pp 423-437.

2007년 7월 30일 원고 접수
2007년 12월 10일 최종 수정본 채택